IEEE Access
Multidisciplinary | Rapid Review | Open Access Journal

Received March 24, 2019, accepted April 12, 2019, date of publication April 16, 2019, date of current version April 26, 2019.

Digital Object Identifier 10.1109/ACCESS.2019.2911549

Compressed Sensing OFDM Time Delay Estimation Based on Atomic Evolution and Elimination

PENG ZHANG[1], WEI-JIA CUI[1], ZI-RU ZHENG[2], AND BIN BA[1]
[1]PLA Strategic Support Force Information Engineering University, Zhengzhou 450001, China
[2]Unit 78118 of PLA, Chengdu 610000, China

Corresponding author: Bin Ba (xidianbabin@163.com)

This work was supported by the National Natural Science Foundation of China under Grant 61401513.

ABSTRACT Aiming at the problem of time delay estimation for orthogonal frequency division multiplexing (OFDM) signals with small samples, a new compressed sensing time delay estimation method based on atomic evolution and elimination is proposed. This method introduces the idea of evolution and elimination from Darwin's evolutionism, abandons the fixed and invariable way of grid points in the traditional algorithm, takes grid points as adjustable parameters, and updates grid points in each iteration process to promote the evolution of atoms. In order to deal with the off-grid effect, the exponential function is directly modified instead of linear approximation, which effectively eliminates the modeling error caused by the original off-grid algorithm. In the process of calculation, the atomic elimination mechanism is adopted, which reduces the amount of calculation and improves the speed of it. The simulation results show that the proposed algorithm can significantly improve the performance of time delay estimation, especially when using coarse grids. Based on the universal software radio peripheral (USRP), the validity of the proposed algorithm is verified by the actual signal.

INDEX TERMS Time delay estimation, orthogonal frequency division multiplexing, compressed sensing, atomic evolution and elimination.

I. INTRODUCTION

Orthogonal frequency division multiplexing (OFDM) technology is gaining attention and application because of its high rate transmission capability and ability to effectively resist frequency selective fading [1]. It has been widely used in various digital transmission and communication systems, such as high-definition digital broadcast television (HDBT), wireless local area network (WLAN) and LTE (long term evolution) etc. Chinese Huawei company also proposes two new basic technologies for 5G air interface, sparse code multiple access (SCMA) and filtering orthogonal frequency division multiplexing (F-OFDM). A large number of applications of OFDM technology have also spawned positioning requirements based on it. Therefore, numerous scholars have studied the positioning techniques based on OFDM signals [2], [3]. The time-delay-based positioning technology has been widely used for its high precision and good stability. The correlation method [4] is a simpler type of delay estimation algorithm. It correlates the backup of the transmitted signal stored locally with the received signal, and determines the delay estimation value according to the peak value of the cross-correlation. However, under the conditions of low signal-to-noise ratio (SNR) and low sampling rate, spectral peak aliasing and even false peaks will occur, which will lead to the decrease of estimation accuracy. High-order cumulant method [5] utilizes the zero characteristic of the high-order cumulant of Gaussian noise to improve the time delay estimation accuracy of non-Gaussian signals effectively, but the algorithm is complex. Maximum likelihood algorithm [6], as a theoretical optimal algorithm, can approach Cramer-Rao Bound (CRB), but its complexity increases exponentially with the dimension of parameters. To solve the problem of high complexity of multi-dimensional search, many optimization algorithms have been proposed, such as importance sampling (IS) [7], Markov chain Monte Carlo (MCMC) [8], and good estimation results have been achieved. Subspace algorithm [9] has been widely used because of its super-resolution property. Its main idea is to get the signal or noise subspace, and

The associate editor coordinating the review of this manuscript and approving it for publication was Ebrahim Bedeer.

then estimate the time delay based on orthogonality or rotation invariance, but it needs full rank of sample covariance matrix for eigen decomposition and multipath number. When the number of samples is small, the covariance matrix is not full rank. Although it can be smoothed in frequency domain, it loses the effective bandwidth [10], which limits the estimation accuracy.

Compressed sensing (CS) is a theory which attracts much attention in recent years. It can recover the sparse signal with a high probability through a small number of observations [11]. CS includes two processes: compression representation and sparse reconstruction. Sparse reconstruction is the core of CS. In [12], the orthogonal matching pursuit (OMP) algorithm is applied to the time delay estimation of impulse radio-ultra wide band (IR-UWB) system, and achieves the estimation of single-path and multi-path delay under the condition of known transmitting signals. Because the greedy algorithm is too greedy, it cannot avoid the influence of the projection of the atoms with smaller energy in the residual error when choosing the atoms with larger energy, and it is based on grid matching, so the estimation accuracy is limited. In [13], to deal with the sparse channel estimation problem of underwater acoustic OFDM, a $l_2 - l_1$ norm-based basis pursuit denoising (BPDN) method is used to obtain better estimation performance than least square (LS) and OMP algorithms. However, the algorithm needs to select regularization parameters.

The estimation of path delay in the above algorithms is based on quantized delay grids, so there will be grid mismatch problem, that is, off-grid effect. Sparse reconstructed delay estimation algorithms are mostly grid-based. Although dense mesh partitioning can compensate for the off-grid effect to a certain extent, it is accompanied by an increase in the dimension of the over-complete dictionary and column correlation. In order to balance the off-grid effect and the complexity of the algorithm, relevant scholars have also studied it. In [14], a sparse reconstruction time delay estimation method using two-stage redundant dictionary is proposed and applied to the time delay estimation of the cumulative pulse contour of pulsars. In [15], a super-resolution compressed sensing algorithm for grid mismatch in line spectrum estimation is proposed, which is based on iterative reweighted approach. Experiments in this paper show that the algorithm achieves super resolution in practical application and is superior to other state-of-the-art algorithms. However, under the condition of low SNR, the strategy of adaptively updating regularization parameter easily leads to the sparse coefficient vectors being too sparse.

Sparse Bayesian Learning (SBL) or Relevant Vector Machines (RVM) [16], has attracted much attention because it can achieve concise representation in machine learning regression and classification. This method uses parameterized automatic relevance determination (ARD) prior [17], which can effectively promote the sparsity of coefficient vectors in the process of solving. Because of its simplicity, flexibility and high reconstruction accuracy, it has been widely used. Its flexibility is mainly embodied in that it can easily incorporate additional parameters into the whole Bayesian inference framework. In [18], to handle the problem of sparse signal reconstruction under multiple measurement vectors (MMV) model, a multiple sparse Bayesian learning (MSBL) algorithm is proposed. The simulation results show that the reconstruction performance of this algorithm is better than that of many new algorithms. In [19], to deal with grid mismatch in direction of arrival (DOA) estimate, a sparse reconstruction method named off-grid sparse Bayesian learning (OGSBL) is proposed. This method reduces the model error by linear approximation of the first order Taylor expansion. However, it cannot bring significant improvement, because the distance between the real value and the nearest grid point remains unchanged in each iteration. Therefore, the estimation accuracy is limited. For the downlink channel estimation problem of frequency-division duplexing (FDD) massive multi-input multi-output (MIMO) systems, a SBL method is proposed in [20] to achieve sparse channel recovery and off-grid refinement. The in-exact block majorize-minimization (MM) algorithm is used to iteratively refine the grid points. And the fixed step size method is used to modify the grid parameters to minimize the off-grid interval, thereby improving the channel recovery performance.

Aiming at the problem of time delay estimation for OFDM systems with small sample size, a novel algorithm based on atomic evolution and elimination (AEE) is proposed. This method introduces the idea of evolution and elimination from Darwin's evolutionism. It can effectively reduce the off-grid effect and eliminate the modeling error caused by the original off-grid algorithm. The simulation results show that the proposed algorithm can significantly improve the performance of time delay estimation, especially when using coarse grids. The main contribution of this paper are exhibited as follows:

1) We provide a novel off-grid model for OFDM time delay estimation. It is a dynamic grid method which abandons the fixed and invariable way of grid points in the original algorithm, takes grid points as adjustable parameters, and updates the grid points in each iteration process to promote the evolution of atoms.

2) We adopt the atomic elimination mechanism, which reduces the amount of calculation and improves the reconstruction speed to achieve real-time processing.

The remainder of this paper is arranged as follows. Section II lists the notations used in the paper. Section III introduces the signal model. Section IV describes the design of the proposed algorithm. Section V is the analysis of complexity and global and local minima. Section VI is the simulation experiments and the actual signal test, which proves the effectiveness of the proposed algorithm. And the conclusion of this paper is in Section VII.

II. NOTATIONS

In this section, some mathematical notations that will be used through this paper are listed in Table 1.

TABLE 1. Mathematical notations.

Notation	Explanation
$\mathbf{I}_N$	$N \times N$ identity matrix
$\mathbf{0}_{M\times N}$	$M \times N$ zero matrix
$(\bullet)^*$	conjugate
$(\bullet)^{\mathrm{T}}$	transpose
$(\bullet)^{\mathrm{H}}$	conjugate transpose
$\mathrm{tr}(\bullet)$	the trace of a matrix
$\mathrm{Re}(\bullet)$	the real part of a matrix or vector
$\mathrm{Im}(\bullet)$	the imaginary part of a matrix or vector
$E(\bullet)$	the mathematical expectation
$\odot$	Hadamard product
$\mathrm{diag}(a_1, a_2, \cdots a_M)$	diagonal matrix with diagonal elements being $a_1, a_2, \cdots a_M$
$\mathbf{A}_{i\bullet}, \mathbf{A}_{\bullet i}, \mathbf{A}_{ij}$	denote the ith row, the ith column and the element that lies in the ith row and the jth column respectively

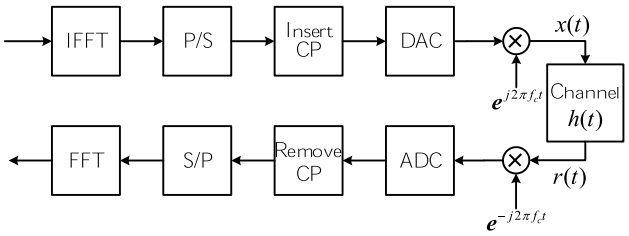

FIGURE 1. The delay estimation block diagram of OFDM signal.

III. SIGNAL MODEL

A. OFDM SYSTEM MODEL

We consider the OFDM system shown in Fig. 1. P/S refers to parallel-to-serial conversion and S/P refers to serial-to-parallel conversion. The system adds cyclic prefix (CP) to eliminate inter-symbol interference (ISI) and inter-channel interference (ICI). An OFDM symbol period is T and the length of CP is longer than the maximum delay spread of the channel i.e.$T_{cp} \geqslant \tau_{\max}$. The carrier frequency is f_c and there are N_{sc} subcarriers, then the system bandwidth is $B = N_{sc}/T$.

In wireless location scenarios, the radio propagation channel under multipath conditions is usually modeled as the complex baseband impulse response (CIR) given by the following formula.

$$h(t,\tau) = \sum_{i=1}^{L} \alpha_i(t)\delta(t - \tau_i(t)), \tag{1}$$

where L is the number of multipath, $\tau_i(t)$ is the propagation delay corresponding to the ith path at time t and all paths are not correlated with each other. $\alpha_i(t) = |a_i(t)|\, e^{j\theta_i(t)}$ is the complex fading coefficient of the ith path at time t, it is a wide stationary narrowband complex Gauss process with Jake's power spectrum [21]. $\delta(\bullet)$ is a Dirichlet function.

During each OFDM symbol transmission, the channel is assumed to be static. Then after channel transmission, removal of CP and discrete Fourier transform (DFT), the received signal $\mathbf{r} = [r(1), r(2), \ldots, r(N_{sc})]^{\mathrm{T}} \in \mathbb{C}^{N_{sc}\times 1}$ can be denoted by

$$\mathbf{r} = \mathbf{X}\mathbf{h} + \mathbf{w} = \mathbf{X}\mathbf{F}\boldsymbol{\alpha} + \mathbf{w}, \tag{2}$$

where $\mathbf{X} = \mathrm{diag}(x(1), x(2), \ldots, x(N_{sc}))$ denotes the transmitted symbols in frequency domain. $\mathbf{h} \in \mathbb{C}^{N_{sc}\times 1}$ is the channel frequency response (CFR) vector. $\mathbf{w} \in \mathbb{C}^{N_{sc}\times 1}$ is typically assumed to be a complex white Gaussian random vector with zero mean and covariance matrix $\sigma_{\mathbf{w}}^2\mathbf{I}$. $\mathbf{F}$ is a partial Fourier matrix satisfying the following form.

$$\mathbf{F} = \frac{1}{\sqrt{N_{sc}}} \times \begin{bmatrix} 1 & cdots & 1 \\ e^{-j2\pi\Delta f\tau_1} & \cdots & e^{-j2\pi\Delta f\tau_L} \\ \vdots & \ddots & \vdots \\ e^{-j2\pi(N_{sc}-1)\Delta f\tau_1} & \cdots & e^{-j2\pi(N_{sc}-1)\Delta f\tau_L} \end{bmatrix} \in \mathbb{C}^{N_{sc}\times L} \tag{3}$$

And the vector of complex fading coefficient is $\boldsymbol{\alpha} = [\alpha(1), \alpha(2), \ldots, \alpha(L)]^{\mathrm{T}} \in \mathbb{C}^{L\times 1}$.

In OFDM systems, channel estimation can be achieved by transmitting pilot sequences over subcarriers. The subcarriers for transmitting pilot may be specified according to the circumstances. For convenience, we define the following set of subscripts to represent the serial number of subcarriers which are used to transmit pilot sequences.

$$\mathcal{P} = \{p(1), p(2), \ldots, p(M)\} \subset \{1, 2, \ldots, N_{sc}\} \tag{4}$$

We select M subcarriers from N_{sc} subcarriers to transmit pilot sequences. And then based on (2), we can get the CFR coefficients of the subcarriers transmitting pilot sequences as follows:

$$\bar{h}(m) = \frac{r(p(m))}{x(p(m))}, \quad m = 1, 2, \ldots, M \tag{5}$$

Then CFR estimation can be expressed as

$$\bar{\mathbf{h}} = (\mathbf{X}_{\mathcal{P}})^{-1}\mathbf{r}_{\mathcal{P}} = \mathbf{h} + (\mathbf{X}_{\mathcal{P}})^{-1}\mathbf{w}_{\mathcal{P}} = \mathbf{F}\boldsymbol{\alpha} + \mathbf{e}, \tag{6}$$

where $\bar{\mathbf{h}} = [\bar{h}(1), \bar{h}(2), \ldots, \bar{h}(M)]^{\mathrm{T}} \in \mathbb{C}^{M\times 1}$. We assume that all pilot sequences are unit power, so the statistical characteristics of the noise term $\mathbf{e} = (\mathbf{X}_{\mathcal{P}})^{-1}\mathbf{w}_{\mathcal{P}}$ remain unchanged.

B. CS THEORETICAL MODEL

The goal of CS sparse reconstruction is to reconstruct the sparse coefficient vector based on the observation vector and the determined sensing matrix. The model is as follows

$$\mathbf{y} = \boldsymbol{\Phi}\mathbf{x} + \mathbf{n}, \tag{7}$$

where $\mathbf{y} \in \mathbb{C}^{M\times 1}$ is the observation vector and $\mathbf{n} \in \mathbb{C}^{M\times 1}$ is the additive complex Gauss white noise. Matrix $\boldsymbol{\Phi} \in \mathbb{C}^{M\times N}$ is a sensing matrix, and the number of its columns is much larger than the number of rows i.e. $N \gg M$. $\mathbf{x} \in \mathbb{C}^{N\times 1}$ is an unknown sparse coefficient vector, and only a few non-zero values are distributed in unknown locations.

Generally, the solution of sparse coefficient vector can be transformed into a quadratic constrained optimization problem based on l_1 norm.

$$\hat{\mathbf{x}} = \underset{\mathbf{x}}{\mathrm{argmin}}\{\|\mathbf{y} - \boldsymbol{\Phi}\mathbf{x}\|_2^2 + \kappa\|\mathbf{x}\|_1\}, \tag{8}$$

where $\kappa > 0$ is called regularization parameter to control the sparsity of sparse vectors. $\|\bullet\|_p$ denotes the l_p norm of a vector. This optimization problem is also known as the basis pursuit denoising (BPDN) [22] or the least absolute shrinkage and selection operator (LASSO) [23] algorithm.

Another method is sparse Bayesian learning (SBL) algorithm. The idea is to find a maximum posteriori (MAP) estimate of sparse coefficient vector $\mathbf{x}$.

$$\hat{\mathbf{x}} = \underset{\mathbf{x}}{\operatorname{argmin}}\{\|\mathbf{y} - \Phi\mathbf{x}\|_2^2 + \lambda^{-1}Q(\mathbf{x})\}, \tag{9}$$

where λ is the inverse of noise variance. By assuming that the sparse coefficient vector satisfies the prior probability distribution $p(\mathbf{x})$, the penalty term $Q(\mathbf{x}) \propto^e -\log p(\mathbf{x})$ (Here $x \propto^e y$ denotes $\exp(x) = \exp(v)\exp(y)$, so for any constant v, there is $x = v + y$) is used to generate the sparse estimate of $\mathbf{x}$.

In the actual signal space, most channel coefficients are zero or close to zero, and only a few multipath are included, so the distribution of the delay values of multipath signals in a certain time domain is sparse.

In order to apply the theory of CS sparse reconstruction to time delay estimation, the model of (6) needs to be processed and the corresponding sparse representation model is constructed. In solving the problem of (7), the columns of matrices $\mathbf{\Phi}$ are known, while the columns of matrices $\mathbf{F}$ in (6) depend on unknown delays $\boldsymbol{\tau} = \{\tau_1, \tau_2, \ldots, \tau_L\}$. To avoid this difference, we introduce a uniformly distributed grid set over a time-delay interval $[0, T]$.

$$\bar{\boldsymbol{\tau}} = \{\bar{\tau}_1, \bar{\tau}_2, \ldots, \bar{\tau}_N\} = \{0, \tfrac{T_s}{\varsigma}, \tfrac{2T_s}{\varsigma}, \ldots, T\}, \tag{10}$$

where $\varsigma > 0$ is a normal number. Assuming that the delay interval $[0, T]$ covers all possible multipath signal delay values in this scenario and the interval between two adjacent delay values is defined as resolution $r = |\bar{\tau}_{i+1} - \bar{\tau}_i|$. Next, we generate atoms according to the partitioned grid to form an over-complete DFT dictionary $\mathbf{V}$.

$$\mathbf{V} = [\mathbf{v}(\bar{\tau}_1), \mathbf{v}(\bar{\tau}_2), \ldots, \mathbf{v}(\bar{\tau}_N)] \in \mathbb{C}^{M\times N} \tag{11}$$

$$\mathbf{v}(\bar{\tau}_i) = \frac{1}{\sqrt{M}}\begin{bmatrix} 1 \\ e^{-j2\pi\Delta f\bar{\tau}_i} \\ \vdots \\ e^{-j2\pi(M-1)\Delta f\bar{\tau}_i} \end{bmatrix} \in \mathbb{C}^{M\times 1} \tag{12}$$

Each column of DFT dictionary $\mathbf{V}$ is called atom and the number of columns is $N = \varsigma T/T_s + 1$. In order to meet the sparsity requirement, there should be $N \gg M > L$. Then the sparse coefficient vector $\bar{\boldsymbol{\alpha}} = [\bar{\alpha}(1), \bar{\alpha}(2), \ldots, \bar{\alpha}(N)]^{\mathrm{T}} \in \mathbb{C}^{N\times 1}$ is defined, and its element value satisfies the requirement.

$$\bar{\alpha}_m(t) = \begin{cases} \alpha_k(t), & \bar{\tau}_m = \tau_k \in \boldsymbol{\tau} \\ 0, & otherwise \end{cases} \tag{13}$$

The above formula also shows that there is a one-to-one relationship between the position of non-zero elements in sparse coefficient vector $\bar{\boldsymbol{\alpha}}$ and the delay value of multipath component of the signal. Only by obtaining the index value of L nonzero elements in $\bar{\boldsymbol{\alpha}}$, the delay estimation value of multipath signal can be obtained.

Then the CS sparse reconstruction model of (6) can be expressed as

$$\bar{\mathbf{h}} = \mathbf{V}\bar{\boldsymbol{\alpha}} + \mathbf{e} \tag{14}$$

C. OFF-GRID MODEL

We have observed that there are natural quantization errors in the grid-based method of time delay, and the final performance is acceptable when the quantization delay value (i.e. resolution) is relatively small. But the performance will be greatly affected when the quantization delay value is relatively large.

In order to compensate for the mesh errors, [24] proposes to use the first-order Taylor expansion to calibrate the mismatch of the mesh. The actual multipath delay values in (14) are respectively $\tau_i \in \boldsymbol{\tau}$. Assuming that the quantization delay value is $\bar{\tau}_{n_i} \in \bar{\boldsymbol{\tau}}$, the Fourier vector $\mathbf{v}(\tau_i)$ corresponding to the actual multipath delay value are expanded to the nearest quantization delay value $\bar{\tau}_{n_i}$, and the following expressions are obtained

$$\mathbf{v}(\tau_i) \approx \mathbf{v}(\bar{\tau}_{n_i}) + \mathbf{d}(\bar{\tau}_{n_i})(\tau_i - \bar{\tau}_{n_i}), \tag{15}$$

where $\mathbf{d}(\bar{\tau}_{n_i}) = \frac{d\mathbf{v}(\tau)}{d\tau}\Big|_{\tau=\bar{\tau}_{n_i}}$ is the first derivative vector of $\mathbf{v}(\tau)$ to τ in the following form

$$\mathbf{d}(\tau_i) = \frac{d\mathbf{v}(\tau_i)}{d\tau_i} = [0 \ -j2\pi\Delta f e^{-j2\pi\Delta f\tau_i} \ \cdots \ -j2\pi\Delta f\,(M-1)\,e^{-j2\pi\Delta f(M-1)\tau_i}]^{\mathrm{T}} \tag{16}$$

The over-complete matrix consisting of the derivative vectors of Fourier vectors $\mathbf{v}(\bar{\tau}_i)$ corresponding to each delay value in set $\bar{\boldsymbol{\tau}}$ is

$$\mathbf{\Psi} = [\mathbf{d}(\bar{\tau}_1), \mathbf{d}(\bar{\tau}_2), \ldots, \mathbf{d}(\bar{\tau}_N)] \in \mathbb{C}^{M\times N} \tag{17}$$

Then the modified over-complete dictionary with time-delay domain sparse expansion and contains off-grid parameters is

$$\mathbf{\Phi}(\boldsymbol{\varphi}) = \mathbf{V} + \mathbf{\Psi}\mathrm{diag}(\boldsymbol{\varphi}), \tag{18}$$

where matrix $\boldsymbol{\varphi} = [\varphi_1, \varphi_2, \ldots, \varphi_N]^{\mathrm{T}} \in [-\frac{r}{2}, \frac{r}{2}]^N$ is an off-grid parameter vector and $\varphi_i = \tau_i - \bar{\tau}_{n_i}$, $i = 1, \ldots, N$.

Then the single measurement vector (SMV) model of (14) can be expressed as

$$\bar{\mathbf{h}} = \mathbf{\Phi}(\boldsymbol{\varphi})\bar{\boldsymbol{\alpha}} + \mathbf{e} \tag{19}$$

Correspondingly, when we can obtain more than one CFR sample, the received signal matrix under the multiple measurement vectors (MMV) model is as follows:

$$\mathbf{H} = \mathbf{\Phi}(\boldsymbol{\varphi})\mathbf{A} + \mathbf{E} \tag{20}$$

where $\mathbf{H} = [\bar{\mathbf{h}}_1, \bar{\mathbf{h}}_2, \ldots, \bar{\mathbf{h}}_K] \in \mathbb{C}^{M\times K}$ is a matrix consisting of K CFR samples. $\mathbf{A} = [\bar{\boldsymbol{\alpha}}_1, \bar{\boldsymbol{\alpha}}_2, \ldots, \bar{\boldsymbol{\alpha}}_K] \in \mathbb{C}^{N\times K}$ is the channel complex fading sparse coefficient matrix, which is joint sparse (or row sparse), that is, all columns in the matrix are sparse vectors, and have the same support set (i.e., the positions of non-zero elements are the same). $\mathbf{E} = [\mathbf{e}_1, \mathbf{e}_2, \ldots, \mathbf{e}_K] \in \mathbb{C}^{M\times K}$ is the noise matrix.

IV. CS DELAY ESTIMATION ALGORITHM BASED ON AEE

In the traditional dictionary-based CS sparse reconstruction model, once atoms are generated according to the partitioned grid, the atoms will not change. But the generated atoms are not exactly the optimal component of the observation vector, that is, the actual delay value is not necessarily just on the grid point. Therefore, the off-grid algorithm is proposed [19]. From the off-grid model in Section III.C, it can be seen that the main idea is to use the first-order Taylor expansion to correct the over-complete dictionary, and then the final estimate is to add the off-grid correction value on the basis of the grid estimation value. However, it should be noted that the distance between the actual delay value and the grid estimation value is constant throughout the iteration process, that is, the model error generated by equation (15) always exists, which limits its estimation accuracy. And in the process of iteration, the irrelevant atoms always participate in the calculation, resulting in too long operation time and too much computation.

The idea of evolution and elimination comes from Darwin's theory of evolution. In nature, through the fierce competition for survival, organisms survive and the unsuitable are eliminated, which is natural selection [25]. This paper is based on the idea of evolution and elimination. In the iterative process of SBL algorithm, atoms evolve continuously to fit in with the components of observation vectors (i.e. adapting to the 'environment'). And when the minimum value of sparse coefficient is less than the elimination threshold (i.e. species that are not suitable for the environment), the elimination mechanism is initiated.

A. THE SPARSE BAYESIAN LEARNING

Thanks to the automatic relevance determination (ARD) method adopted by SBL, the hyperparameters can be adaptively learned from the observed data to realize the evolution of atoms. ARD results in a sparse solution at each iteration, which results in efficient global competition among all possible values of sparse coefficients. It was first applied to determine the selection of input variables of neural networks [26]. When many input variables are added to the neural network on the basis of the principle of equality, the limited number of training samples will lead to the occasional occurrence of irrelevant input, and ultimately the prediction performance will be poor. Therefore, if it does contain a large number of potentially unrelated inputs, asymmetric priori must be used and the degree of correlation of unknown inputs can be automatically determined in training.

1) A PRIORI HYPOTHESIS

From (20), the MMV model of CFR matrix with off-grid parameters can be obtained.

$$\mathbf{H} = \mathbf{\Phi A} + \mathbf{E} \tag{21}$$

We use a prior distribution to make probability assumptions about the unknown variables in the signal model.

Assuming that the potential arrival paths represented by each row of sparse coefficient matrix $\mathbf{A}$ in (21) are independent, and that each row of data satisfies a complex Gaussian distribution with zero mean $\mathbf{0}_{1\times K}$ and covariance matrix $\gamma_i\mathbf{I_K}$.

$$p(\mathbf{A}_{i\bullet};\gamma_i) = \mathrm{CN}(\mathbf{0}_{1\times K}, \gamma_i\mathbf{I_K}), \quad i = 1,\ldots,N \tag{22}$$

The non-negative hyperparameters in vector $\boldsymbol{\gamma} = [\gamma_1, \gamma_2, \ldots, \gamma_N]^{\mathrm{T}}$ controls the row sparsity of sparse coefficient matrix $\mathbf{A}$, i.e. if $\gamma_i \to 0$, then $\mathbf{A}_{i\bullet} \to \mathbf{0}_{1\times K}$.

For the noise matrix $\mathbf{E} \in \mathbb{C}^{M\times K}$, assuming that it satisfies the complex Gaussian distribution, the probability density function is

$$p(\mathbf{E}|\lambda) = \prod_{t=1}^{K} \mathrm{CN}(\mathbf{0}_{M\times 1}, \lambda^{-1}\mathbf{I}_M), \tag{23}$$

where $\lambda = \sigma^{-2}$ is the inverse of noise variance.

In the sparse extension of time-delay domain, the time-delay interval is evenly divided into a set of discrete points. Similar to uniformly partitioned grid points, we also assume that the off-grid parameters are uniformly distributed, and the probability distribution is as follows

$$p(\boldsymbol{\varphi}) = \prod_{n=1}^{N} \mathrm{U}(\varphi_n|[-\tfrac{r}{2}, \tfrac{r}{2}]) \tag{24}$$

2) BAYESIAN INFERENCE

The maximum posteriori probability density of each column of sparse coefficient $\mathbf{A}$ is

$$p(\mathbf{A}_{\bullet j}|\mathbf{H}_{\bullet j}, \mathbf{\Lambda}) = \mathrm{CN}(\boldsymbol{\mu}_j, \mathbf{\Sigma_A}), \quad j = 1,\ldots,K \tag{25}$$

Then the maximum posterior mean matrix $\mathbf{\Pi}$ and covariance matrix $\mathbf{\Sigma_A}$ of matrix $\mathbf{A}$ are expressed as

$$\mathbf{\Pi} = \mathbf{\Lambda\Phi}^{\mathrm{H}}(\lambda\mathbf{I}_M + \mathbf{\Phi\Lambda\Phi}^{\mathrm{H}})^{-1}\mathbf{H} \tag{26}$$

$$\mathbf{\Sigma_A} = (\mathbf{\Lambda}^{-1} + \lambda^{-1}\mathbf{\Phi}^{\mathrm{H}}\mathbf{\Phi})^{-1} \tag{27}$$

where $\mathbf{\Lambda} = \mathrm{diag}[\boldsymbol{\gamma}]$ is a diagonal matrix composed of vector $\boldsymbol{\gamma} = [\gamma_1, \gamma_2, \ldots, \gamma_N]^{\mathrm{T}}$ and $\mathbf{\Pi} = [\boldsymbol{\mu}_1, \ldots, \boldsymbol{\mu}_K]$ is a maximum posterior mean matrix.

In order to solve the hyperparameters, we use expectation maximization (EM) algorithm. In E step, the posterior parameters need to be solved by using (26) and (27); In M step, the hyperparameters need to be updated, and their iteration formulas are as follows [18].

$$\gamma_i \leftarrow \frac{1}{K}\mathbf{\Pi}_{i\bullet}\mathbf{\Pi}_{i\bullet}^{\mathrm{H}} + (\mathbf{\Sigma_A})_{ii}, \quad i = 1,\ldots,N \tag{28}$$

$$\lambda \leftarrow \frac{\|\mathbf{H} - \mathbf{\Phi\Pi}\|_{\mathrm{F}}^2 + \lambda K\,\mathrm{tr}[\mathbf{\Phi\Lambda\Phi}^{\mathrm{H}}(\lambda\mathbf{I}_M + \mathbf{\Phi\Lambda\Phi}^{\mathrm{H}})^{-1}]}{MK} \tag{29}$$

For off-grid parameters, their values can be obtained by solving the following optimization problems

$$\boldsymbol{\varphi} \leftarrow \arg \min_{\boldsymbol{\varphi}\in[-\frac{r}{2},\frac{r}{2}]^N} \{\boldsymbol{\varphi}^{\mathrm{T}}\mathbf{\Omega\varphi} - 2\boldsymbol{\upsilon\varphi}\} \tag{30}$$

where the expressions of matrix $\mathbf{\Omega}$ and vector $\boldsymbol{\upsilon}$ are respectively as follows [19].

$$\mathbf{\Omega} = \mathrm{Re}\left\{\Psi^{\mathrm{T}}\Psi^{*} \odot \left(\frac{1}{K}\mathbf{\Pi}\mathbf{\Pi}^{\mathrm{H}} + \mathbf{\Sigma}_{\mathbf{A}}\right)\right\} \tag{31}$$

$$\boldsymbol{\upsilon} = \mathrm{Re}\left\{\frac{1}{K}\sum_{t=1}^{K}\mathrm{diag}(\mathbf{\Pi}_{\bullet t}^{*})\Psi^{\mathrm{H}}(\mathbf{H}_{\bullet t} - \mathbf{V}\mathbf{\Pi}_{\bullet t})\right\} - \mathrm{Re}\left\{\mathrm{diag}(\Psi^{\mathrm{H}}\mathbf{V}\Sigma_{\mathbf{A}})\right\} \tag{32}$$

Equation (30) derives $\boldsymbol{\varphi}$, and we can get the solution of it, $\boldsymbol{\varphi} = \mathbf{\Omega}^{-1}\boldsymbol{\upsilon}$. But if $\mathbf{\Omega}$ is not invertible, i.e. singular, it cannot be solved in this way. Instead, it should be solved by iteration step by step. As the iterative algorithm for singular linear equations in [27]. And the formula is as follows:

$$\hat{\varphi}_i = \frac{\boldsymbol{\upsilon}_i - (\mathbf{\Omega}_{\bullet i})^{\mathrm{T}}_{-i}\boldsymbol{\varphi}_{-i}}{\mathbf{\Omega}_{ii}}, \tag{33}$$

where $\mathbf{u}_{-i}$ denotes the vector formed after removing the ith element of the vector $\mathbf{u}$.

Similar to the original SBL algorithm, EM algorithm is still used to solve the above-mentioned hyperparameters. Because of the characteristics of EM algorithm [28], AEESBL algorithm can guarantee convergence.

B. ATOMIC EVOLUTION AND ELIMINATION

A column in an over-complete dictionary is called an atom. For signals that can be sparsely represented, it consists of the weighted sum of only a few atoms in an over-complete dictionary whose column numbers are called support sets. According to the CS theoretical model in Section III.B, we divide a time-delay interval evenly to generate atoms, and then form an over-complete dictionary. In fact, there are modeling errors in this step, because there is no guarantee that the generated atoms contain the optimal constituent atoms of the observed data. For an atom that does not constitute observation data, its weight coefficient is zero. However, under noisy conditions, after sparse reconstruction, the weight coefficients of unrelated atoms are not zero, but tend to be smaller values. And during the reconstruction process, the existence of extraneous atoms increases the amount of computation.

This paper is based on the fact that the generated atom is not necessarily the optimal atom and the increase of the computational quantity because of the unrelated atoms, thus introducing the idea of evolution and elimination. In the iterative process of SBL algorithm, let atoms evolve and eliminate.

1) ATOMIC EVOLUTION

In the Bayesian inference of Section IV.A, from the expressions (26), (27), (29), (31) and (32), it can be seen that the revised over-complete dictionary $\mathbf{\Phi}$, DFT over-complete dictionary $\mathbf{V}$ and its derivative dictionary $\mathbf{\Psi}$ are all involved in the solving process of the algorithm. In the traditional off-grid SBL algorithm, the dictionary $\mathbf{V}$ and $\mathbf{\Psi}$ are fixed. Atomic estimation schematic diagram of traditional off-grid SBL algorithm is shown in Fig. 2, in which the dotted line

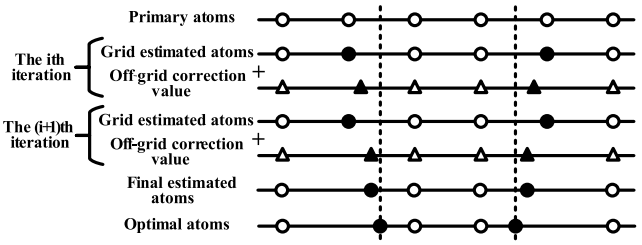

FIGURE 2. Atomic estimation process diagram of traditional off-grid SBL algorithm.

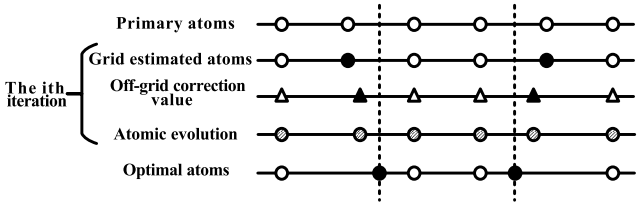

FIGURE 3. Atomic evolution diagram.

passing through the black circle represents the optimum atom composition of the observed data. The primary atoms represent column vectors in the DFT dictionary. In this line with the word 'grid estimated atoms', the black circle represents the atom that best matches the observed data obtained in the primary atoms. In the line with the word 'off-grid correction value', the black triangle represents the off-grid correction based on the most matched atom of the grid estimation, and the white triangle represents the correction value is zero. Then the final atom is the grid estimate atom plus the off-grid correction.

The primary atom is an exponential function form with a high degree of nonlinearity. From the linear approximation of the optimal atom by the first-order Taylor expansion in equation (15), it can be seen that there is an approximation error, which is bound to limit the final delay estimation accuracy. In order to reduce the error caused by this linear approximation and further improve the accuracy of the delay estimation. This paper breaks the idea of fixed atoms and introduces the idea of atomic evolution. Instead of using a linear approximation, the exponential function is directly corrected.

A schematic diagram of atomic evolution is shown in Fig. 3, where the grey circles represent the atoms of evolution. The specific evolution is as follows:

1. In an iterative process, after the off-grid parameter $\boldsymbol{\varphi}$ is obtained, a new grid $\bar{\boldsymbol{\tau}}^{new}$ is obtained according to the current grid $\bar{\boldsymbol{\tau}}^{old}$.

$$\bar{\boldsymbol{\tau}}^{new} - \bar{\boldsymbol{\tau}}^{old} + \boldsymbol{\varphi} \tag{34}$$

2. Then, based on the new delay grid, new atoms are generated and new over-complete dictionaries are constructed.

$$\mathbf{V}^{new} = \left[\mathbf{v}\left(\bar{\tau}_1^{new}\right), \mathbf{v}\left(\bar{\tau}_2^{new}\right), \ldots, \mathbf{v}\left(\bar{\tau}_N^{new}\right)\right] \in \mathbb{C}^{M\times N} \tag{35}$$

$$\boldsymbol{\Psi}^{new} = \left[\mathbf{d}\left(\bar{\tau}_1^{new}\right), \mathbf{d}\left(\bar{\tau}_2^{new}\right), \ldots, \mathbf{d}\left(\bar{\tau}_N^{new}\right)\right] \in \mathbb{C}^{M\times N} \tag{36}$$

$$\boldsymbol{\Phi}^{new} = \mathbf{V}^{new} + \boldsymbol{\Psi}^{new}\mathrm{diag}(\boldsymbol{\varphi}) \tag{37}$$

3. In EM algorithm, the new over-complete dictionaries are used to solve the problem.

By comparing the formulas (11) and (17) with (35) and (36), we can see that the over-complete dictionary atoms in this algorithm are not fixed, but evolve in the process of iteration, which is the advantage of this algorithm.

2) ATOMIC ELIMINATION

In the traditional SBL algorithm, the entire over-complete dictionary will participate in the operation, and the existence of unrelated atoms will not only cause interference to the final result, but also cause a larger data dimension and more computation. In order to reduce the amount of computation and speed up the reconstruction to achieve real-time processing, we introduce a mechanism for atomic elimination.

In the process of Bayesian learning, the value of the non-negative hyperparameters γ_i corresponds to the row sparsity degree of sparse coefficient matrix $\mathbf{A}$. When $\gamma_i \to 0$, there should be $\mathbf{A}_{i\bullet} \to \mathbf{0}_{1\times K}$, and the corresponding atom in the over-complete dictionary should be eliminated. However, since the observation data is noisy, the hyperparameters corresponding to the unrelated atoms are not zero. Therefore, in the actual processing, a relatively small threshold ε is set in advance, and once the minimum γ_i is less than ε, the elimination process will be started. The specific elimination process is as follows:

First define the complete set $\mathbf{S} = \{1, 2, \ldots, N\}$.

1. Before each iteration, a decision is made as to whether the elimination process needs to be initiated. If the elimination condition is met, find the index value of the value in $\boldsymbol{\gamma}$ that is greater than the elimination threshold (i.e. the sequence number of the element in vector $\boldsymbol{\gamma}$);

$$\begin{aligned} &if\ \min(\boldsymbol{\gamma}) < \varepsilon \\ &\quad inde = \arg_i\{\gamma_i > \varepsilon\} \end{aligned} \tag{38}$$

2. Update each variable $\boldsymbol{\gamma} = \boldsymbol{\gamma}_{inde}$, $\mathbf{V} = \mathbf{V}_{\bullet(inde)}$, $\boldsymbol{\Psi} = \boldsymbol{\Psi}_{\bullet(inde)}$, $\boldsymbol{\varphi} = \boldsymbol{\varphi}_{inde}$ and $\mathbf{S} = \mathbf{S}_{inde}$.

C. ALGORITHM STEPS

Through the above analysis, the algorithm steps can be summarized as follows in Algorithm 1.

Algorithm 1 CS Time Delay Estimation Based on AEE

Input: The observation data $\mathbf{H}$, initial time delay grid $\bar{\boldsymbol{\tau}}$, the over-complete DFT dictionary $\mathbf{V}$ and its derivative dictionary $\boldsymbol{\Psi}$, the elimination threshold ε, the termination threshold tol and maximum number of iterations $i_{\max}$;

Steps:

1.Initialize the parameters: $\boldsymbol{\gamma}^{(0)} = \mathbf{1}_{N\times 1}$, $\lambda^{(0)} = \frac{1}{K}\sum_{j=1}^{K}\mathrm{var}(\mathbf{H}_{\bullet j})$, $\boldsymbol{\varphi}^{(0)} = \mathbf{0}_{N\times 1}$ and set $i = 0$;

2.Atomic elimination determination: If the conditions for atomic elimination are met, proceed to the steps in Section IV.B.2). If not, continue execution;

3.Atomic evolution process: Construct a diagonal matrix $\boldsymbol{\Lambda}$ using hyperparameters $\boldsymbol{\gamma}^{(i)}$, construct new delay grids $\bar{\boldsymbol{\tau}}^{(i+1)}$, over-complete DFT dictionary $\mathbf{V}^{(i+1)}$, derivative dictionary $\boldsymbol{\Psi}^{(i+1)}$ and over-complete dictionary $\boldsymbol{\Phi}^{(i+1)}$ with off-grid parameters according to equations (34), (35), (36) and (37) using $\boldsymbol{\varphi}^{(i)}$ and $\bar{\boldsymbol{\tau}}^{(i)}$;

4.Calculate $\boldsymbol{\Pi}$ and $\boldsymbol{\Sigma}_{\mathbf{A}}$ according to equations (26) and (27) respectively;

5.Via (28) to update the hyperparameters $\boldsymbol{\gamma}^{(i)}$, via (29) to update $\lambda^{(i)}$, via (33) to update $\boldsymbol{\varphi}^{(i)}$;

6.If $\left\|\boldsymbol{\gamma}^{(i+1)} - \boldsymbol{\gamma}^{(i)}\right\|_2 / \left\|\boldsymbol{\gamma}^{(i)}\right\|_2 < tol$ or $i = i_{\max}$, the iteration stops; If not, set $i = i + 1$, jump to step 2;

7.Obtain the estimated value of delay according to the following formulas.

$$index = \arg_i nonzero\{\gamma_i\} \tag{39}$$

$$\hat{\boldsymbol{\tau}} = \bar{\boldsymbol{\tau}}_{index} \tag{40}$$

Output: The estimated value of the delay $\hat{\boldsymbol{\tau}}$.

V. ANALYSIS

A. COMPLEXITY ANALYSIS

Since the algorithm in this paper is an iterative class algorithm and has an atomic elimination (i.e. data dimensionality reduction) process, we analyze the amount of computation during each iteration before atomic elimination. As shown in Table 2, where M is the number of subcarriers transmitting pilots, N is the number of over-complete dictionary columns, and K is the number of samples. In the E step of the EM algorithm,

TABLE 2. Computational complexity.

Steps	Main computations	Amount of computation
E-step	$(\lambda\mathbf{I}_M + \boldsymbol{\Phi}\boldsymbol{\Lambda}\boldsymbol{\Phi}^{\mathrm{H}})^{-1}$	$O(M^3 + MN^2 + M^2N)$
M-step	$\boldsymbol{\Omega}$	$O(N^3)$
Total		$O(M^3+N^3+MN^2+M^2N)$

the maximum a posteriori mean matrix $\boldsymbol{\Pi}$ and the covariance matrix $\boldsymbol{\Sigma}_{\mathbf{A}}$ need to be solved, and the main formula is $(\lambda\mathbf{I}_M + \boldsymbol{\Phi}\boldsymbol{\Lambda}\boldsymbol{\Phi}^{\mathrm{H}})^{-1}$; In the M step, the hyperparameters need to be updated, and the main formula is to invert the matrix $\boldsymbol{\Omega}$.

B. ANALYSIS OF GLOBAL AND LOCAL MINIMA

In Bayesian inference of SBL, we can get its cost function as follows:

$$\mathcal{L}(\boldsymbol{\eta}) = K\log|\Sigma_{\mathbf{H}}| + \sum_{j=1}^{K}\mathbf{H}_{\bullet j}^{\mathrm{H}}\Sigma_{\mathbf{H}}^{-1}\mathbf{H}_{\bullet j} \tag{41}$$

where $\Sigma_{\mathbf{H}} = \lambda\mathbf{I}_M + \Phi\Lambda\Phi^{\mathrm{H}}$.

The analysis of the local minima and global minima of the cost function of SBL is given in [29]. The original mathematical model of the proposed algorithm and the method used in

the hyperparameters' solving process are similar to [29]. The difference is that the algorithm in this paper considers that the over-complete dictionary is not fixed, but dynamically revised in the iteration process of the algorithm to compensate for the model error. Therefore, the analysis of the global and local minima of the proposed algorithm can be referred to in [29].

VI. EXPERIMENTS

A. SIMULATION ANALYSIS

In this paper, the time delay estimation algorithm of OFDM signal in wireless positioning system model is studied. The proposed algorithm–AEESBL is compared with the MSBL algorithm in [18], the OGMSBL algorithm in [19], the OGBULA algorithm in [20], the SOMP algorithm in [30] and the SS-MUSIC algorithm in [9] (using frequency-domain smoothing to make the sample covariance matrix full rank). According to the IEEE 802.11a protocol [31], the parameters of the OFDM system are set in the simulation as shown in Table 3.

TABLE 3. System parameters for the experiments.

Simulation Parameters	Value
FFT cycle	$T = 3.2\ \mu s$
System bandwidth	$B = 20$ MHz
Number of subcarriers	$M = 64$
Carrier frequency	$f_c = 2.4$ GHz
Maximum delay spread	$\tau_{\max} = 800$ ns
Number of channel paths	$L = 3$
Power of the paths(normalization)	$[0, -1, -2]$ dB
Number of samples	$K = 10$

To measure the performance of the algorithm, we define the root mean square error (RMSE) for all paths of the delay.

$$\mathrm{RMSE} = \sqrt{\frac{1}{LP}\left(\sum_{p=1}^{P}\sum_{i=1}^{L}\left|\hat{\tau}_{pi} - \tau_{pi}\right|^2\right)} \tag{42}$$

where L is the number of multipath, P is the number of Monte Carlo simulations, $\widehat{\tau}_{pi}$ is the estimated delay value of the ith path in the pth Monte Carlo experiment. And τ_{pi} is the actual delay value of the ith path in the pth Monte Carlo experiment. The equipment used in all simulation experiments is a Win7 system and Intel Xeon CPU (4-core 3.3 GHz) computer.

Simulation 1 (Verifying algorithm validity): In order to verify the performance of the algorithm, set the delay values of the three paths to $\tau_1 = 94.31\ ns$, $\tau_2 = 346.29\ ns$ and $\tau_3 = 626.99\ ns$. The mesh is evenly divided on the delay interval [0, 800] *ns* and the grid interval is 4 *ns*, so the actual delay values are not on the grid points. And the sub-carriers all transmit pilot sequences. The distribution of the delay estimation results is obtained under the conditions of $SNR = 20\ dB$ and $0\ dB$, respectively. As shown in Fig. 4, it can be seen from the figure that the proposed algorithm can effectively estimate the delay.

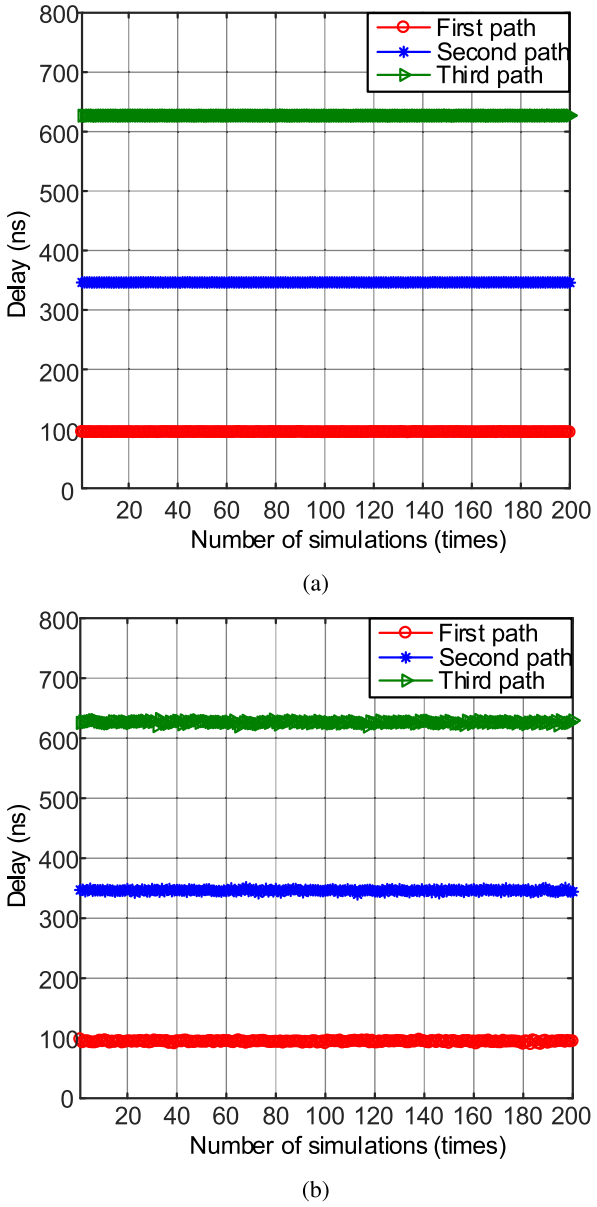

FIGURE 4. Time delay estimation result. (a) SNR=20 dB. (b) SNR=0 dB.

Simulation 2 (Analysis of atomic evolution and elimination process):

In this simulation, we analyze the process of atomic evolution and elimination. The system parameters are the same as Simulation 1. In order to show the process of atomic evolution and elimination in this algorithm, under the condition of $SNR = 20\ dB$, different elimination thresholds are set and a Monte Carlo experiment is carried out respectively. The changes of the grid are output, and then the process diagram of atomic evolution and elimination is drawn as shown in Fig. VI-A. From the six sub-graphs in Fig. VI-A, we can see that the sub-optimal atoms evolve to the optimal atoms, and the irrelevant atoms will be eliminated in the iteration. Comparing the six sub-graphs, we can find that when the

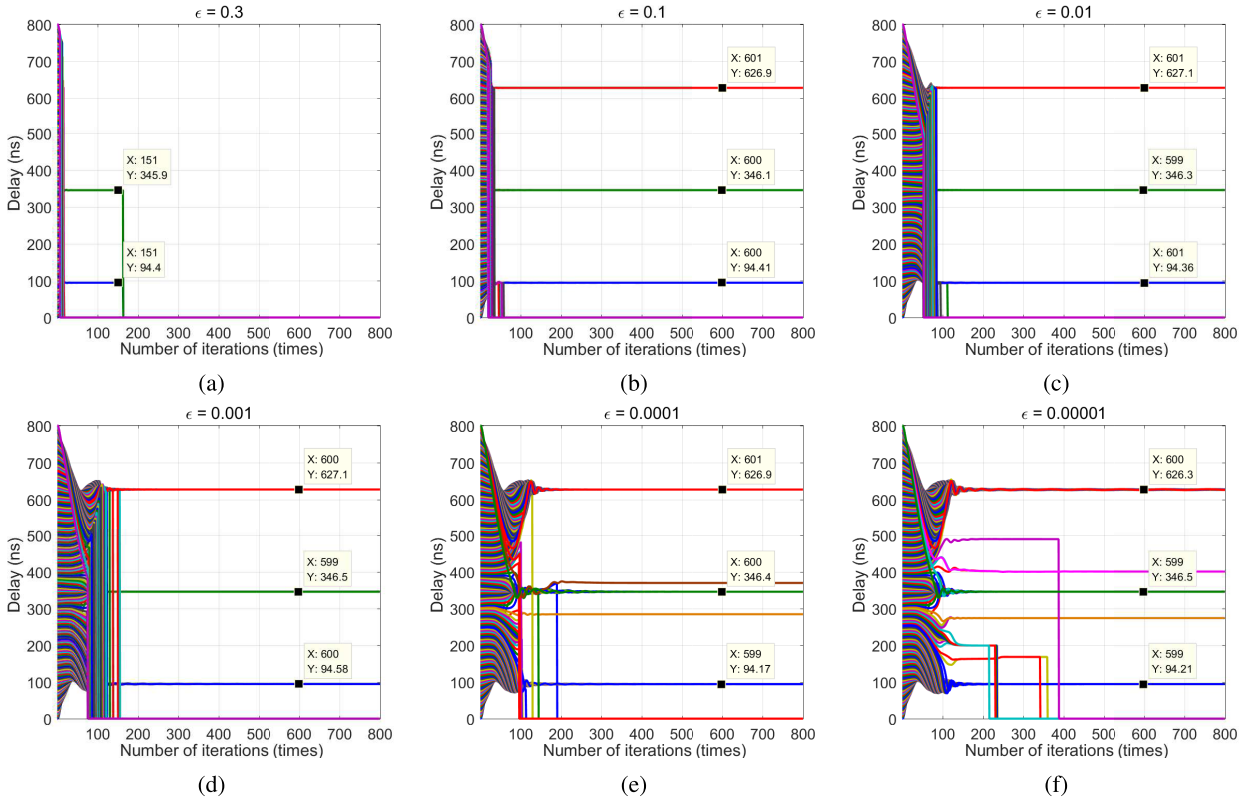

FIGURE 5. Atomic evolution and elimination course. (a) $\varepsilon = 0.3$. (b) $\varepsilon = 0.1$. (c) $\varepsilon = 0.01$. (d) $\varepsilon = 0.001$. (e) $\varepsilon = 0.0001$. (f) $\varepsilon = 0.00001$.

elimination threshold is relatively large, the process of atomic evolution and elimination is faster. While when the threshold is relatively small, the process of evolution and elimination is slower. And the smaller the threshold is, the slower the elimination process and the less complete the elimination will be. Of course, the choice of threshold should not be too big. If too big, it is too likely that the optimal atoms with smaller energy will also be eliminated. As shown in Fig. VI-A(a), the elimination threshold is 0.3 and we find that the third path is also eliminated because of its small energy. Therefore, the selection of elimination threshold needs to be balanced between estimation accuracy and operation time.

Simulation 3 (Comparison of estimated error cumulative distribution functions of different algorithms):

Furthermore, all the subcarriers are set to transmit pilot sequences and the number of Monte Carlo experiment is 200. In each Monte Carlo experiment, the delay values of three paths are randomly generated from the delay intervals $[95, 105]$ *ns*, $[345, 355]$ *ns* and $[625, 635]$ *ns* respectively. The grid interval is 4 *ns*. Under $SNR = 20$ *dB* and 0 *dB* conditions, the cumulative distribution function (CDF) of each algorithm are plotted, as shown in Fig. 6. As can be seen from the figure, the proposed algorithm, OGBULA algorithm and OGMSBL algorithm have smaller estimation error because of the grid modification, which is better than the grid-based algorithm.

Simulation 4 (Estimated performance comparison of different algorithms):

In order to verify the performance of different algorithms for time delay estimation under different SNR conditions, simulation parameters are the same as Simulation 3. SNR ranges from -5 *dB* to 25 *dB*, and grid interval are set to 4 *ns* and 6 *ns*, respectively. The RMSE curves of different algorithms versus SNR are drawn, as shown in Fig. 7. From the graph, we can see that the grid-based algorithm has a flat-bottomed effect at high SNR, that is, RMSE decreases slightly with the increase of SNR. The RMSE of the proposed algorithm, OGBULA algorithm and OGMSBL algorithm decrease significantly with the increase of SNR due to the modification of grid. Under different SNR, the performance of the proposed algorithm is better than that of OGMSBL algorithm. This is because the model error of OGMSBL algorithm is effectively compensated by the evolution of atoms, and the interference of irrelevant atoms is further reduced by using the atomic elimination mechanism, thus the estimation accuracy is effectively improved. Although both the proposed algorithm and OGBULA algorithm adjust the grid parameters, the fixed step size is adopted in OGBULA algorithm, which limits the estimation accuracy.

Simulation 5 (Verify the impact of training pilot number on estimation performance):

The position and number of training pilots can be set in OFDM system. Here, in order to highlight that the sparse reconstruction method of CS can recover the original signal from the dimension-reduced data, the pilot number is changed from 20 to 60, and the position is generated randomly.

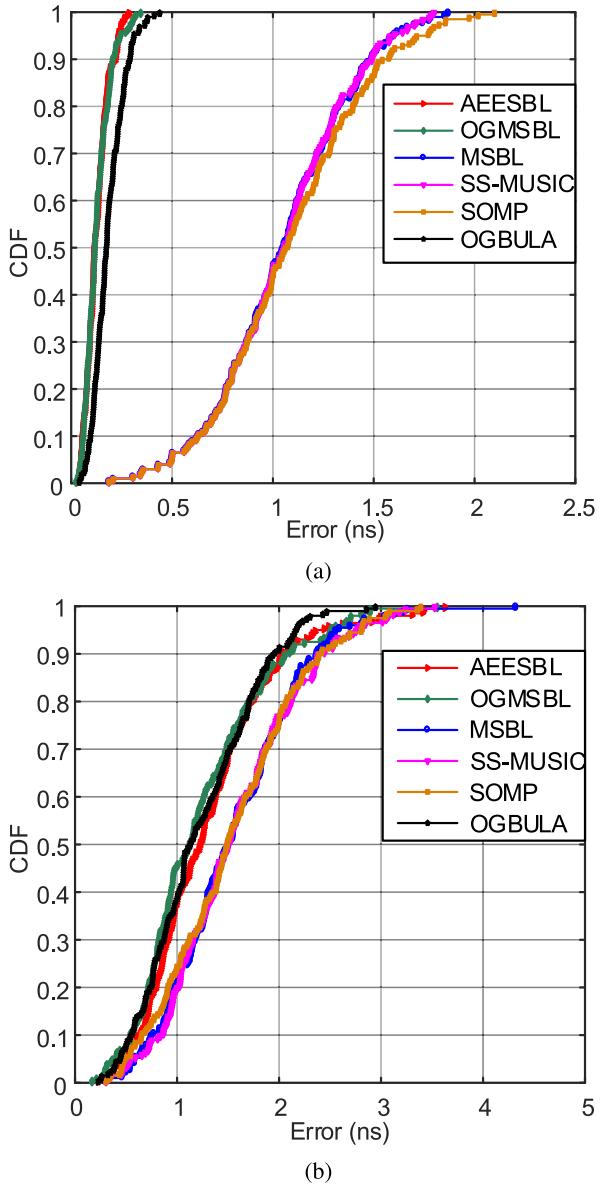

FIGURE 6. Estimation error cumulative distribution function of different algorithms. (a) SNR=20 dB. (b) SNR=0 dB.

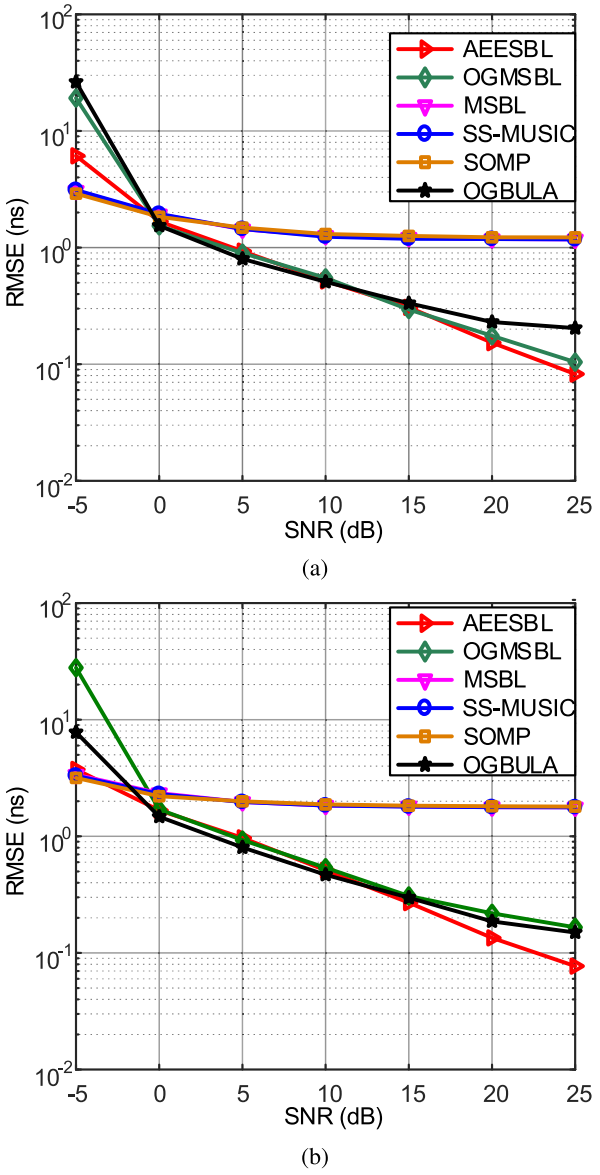

FIGURE 7. The RMSE of different algorithms versus SNR. (a) r=4 ns. (b) r=6 ns.

The RMSE curve of sparse reconstruction algorithm is plotted under the condition of 4 *ns* grid interval and 20 *dB* SNR. However, SS-MUSIC(subspace algorithm) cannot estimate the delay in the case of compressed data and small samples. This is because the partial Fourier matrix do not satisfy the form of Vandermonde matrix after random selection of pilot positions, and the smoothing algorithm is invalid. As shown in Fig. 8, it can be seen from the figure that RMSE of each algorithm decreases with the increase of training pilots, indicating that the estimation accuracy increases with the increase of training pilots. This is because the increase of pilot number is equivalent to the increase of information, so the estimation accuracy will also be improved.

Simulation 6 (Verify the impact of grid interval on estimated performance and computation time):

In order to verify the effect of grid interval on the estimation performance of the algorithm, the grid interval is set to $r = [2, 4, 6, 8, 10]$ *ns* respectively, the number of Monte Carlo is 200, and the SNR is 20 *dB*. In each Monte Carlo experiment, the delay of three paths are randomly generated from the intervals [95, 105] *ns*, [345, 355] *ns* and [625, 635] *ns* respectively. The RMSE curve versus grid interval is obtained as shown in Fig. 9. As can be seen from the graph, the estimation accuracy of the proposed algorithm, OGBULA algorithm and OGMSBL algorithm are higher than that of grid-based algorithms under different grid interval. It also can be found that RMSE of OGMSBL algorithm increases with the increase of grid interval, because the influence of model error increases with the increase of grid interval, which leads to the decrease of estimation accuracy. While the RMSE of the proposed algorithm and OGBULA

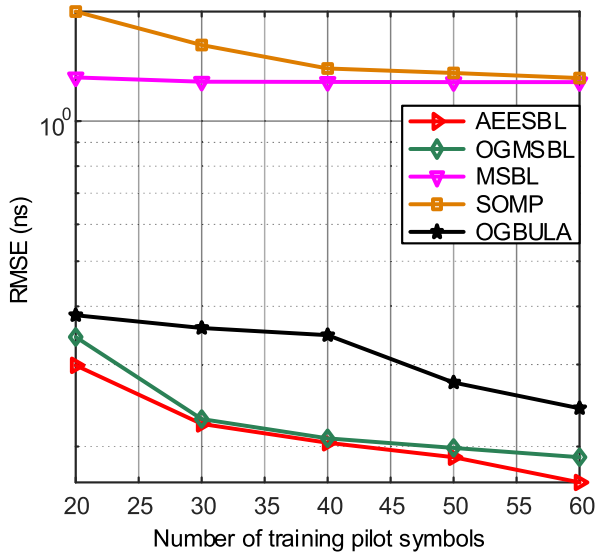

FIGURE 8. The RMSE of different algorithms versus the number of training pilot symbols.

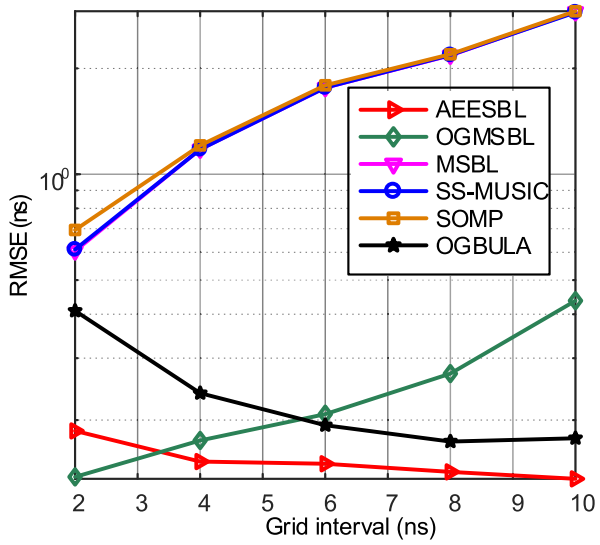

FIGURE 9. The RMSE of different algorithms versus the grid interval.

algorithm decrease with the increase of grid interval, this is because these two algorithms can effectively reduce the model error by adjusting the grid parameters. It can be found that the RMSE of the proposed algorithm and OGBULA algorithm are higher than that of OGMSBL algorithm when the grid interval is small. This is mainly due to the large correlation between atoms when the grid interval is small, which easily makes the grid parameters adjust in the non-optimal direction. When the grid interval is large, the correlation is small. And the advantage of grid parameter adjustment is prominent, so estimated RMSE will decline. It can also be found that the RMSE curve of the proposed algorithm is lower than that of OGBULA algorithm under different grid interval conditions. This is still caused by the fixed step size adjustment of grid parameters in OGBULA algorithm.

We also compare the average running time versus different grid interval of three grid-correction algorithms–OGMSBL algorithm, OGBULA algorithm and the proposed algorithm. The simulation conditions are the same as those of the above experiments. In the three algorithms, the termination threshold is $tol = 1 \times 10^{-8}$ and the maximum number of iterations is $i_{\max} = 800$. In the proposed algorithm, the atomic elimination threshold is $\varepsilon = 0.1$. As shown in Table 4, it can be seen from the table that the average running time of the three algorithms decrease with the increase of the grid interval, because the dimension of the over-complete dictionary decreases. It can be found that the average running time of the proposed algorithm under different grid interval are lower than that of OGMSBL algorithm and OGBULA algorithm, because the proposed algorithm uses atomic elimination mechanism, which reduces the data dimension and improves the operation speed.

TABLE 4. Average CPU time of different algorithms versus the grid interval Time unit (sec).

Algorithms	$r = 2$ ns	$r = 4$ ns	$r = 6$ ns	$r = 8$ ns	$r = 10$ ns
OGMSBL	34.7902	8.7235	5.3321	3.8224	2.9256
OGBULA	7.7370	2.3122	2.1343	2.0804	2.0489
AEESBL	3.9166	0.7088	0.2166	0.1531	0.1529

B. ACTUAL SIGNAL TEST

We use the WLAN-OFDM signal receiving routine (sdruwlanofdm80211BeaconRx.m) based on the universal software radio peripheral (USRP) in MATLAB 2017 to estimate the actual time delay of the OFDM signal. This example in MATLAB 2017 can use USRP devices to implement WLAN receivers, and can give channel estimation results for two MAC address communications. Based on this, the proposed algorithm can be used to estimate the signal propagation delay between the two communication nodes, and then the distance can be estimated. The validity of the proposed algorithm is verified by comparing the actual distance with the estimated distance.

Fig. 10 is a scene diagram for actual signal acquisition. On a standard track and field 100-meter runway, the receiving end is located at the starting point of the runway, and the transmitting end moves from 50m to 100m from the receiving end, with a stepping distance of 10 m. Each test point collects 10 consecutive time channel estimation results, and the delay estimation under small sample conditions is respectively performed for each group of CFR. In the IEEE 802.11a

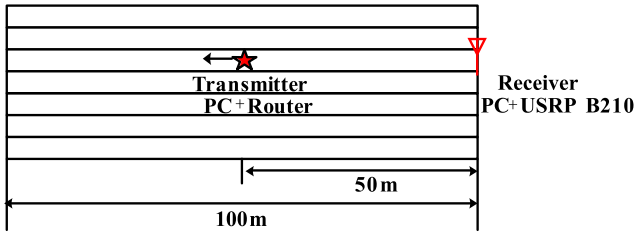

FIGURE 10. The photograph of actual test scene.

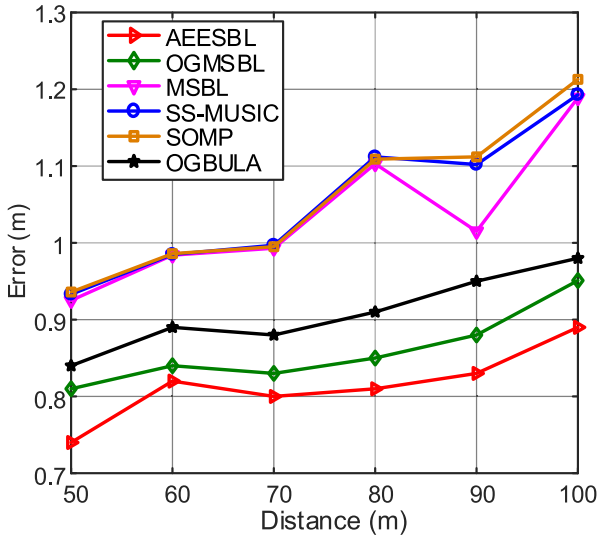

FIGURE 11. Comparison of estimation errors in actual signal testing.

protocol [27], the number of subcarriers actually used is 52, wherein subcarriers $1 \sim 26$ correspond to IFFT inputs of the same label; Subcarriers $-26 \sim -1$ correspond to IFFT inputs of $38 \sim 63$; The next $27 \sim 37$ and port 0 are null. Then, in the simulation, the occupied pilot position is set according to the protocol.

Fig. 11 is a comparison of the estimated average error of several algorithms for the direct path. The grid interval is set to $4ns$. It can be seen from the figure that the algorithm has better performance in the actual signal delay estimation.

VII. CONCLUSIONS

This paper proposes a CS time delay estimation algorithm based on atomic evolution and elimination. It introduces the idea of evolution and elimination, and uses grid points as tunable parameters. The grid points are updated during each iteration to facilitate the evolution of the atom. And the atomic elimination mechanism is adopted to remove the less relevant atoms from the over-complete dictionary, thereby reducing the calculation amount and improving the operation speed. The simulation results show that the proposed algorithm can significantly improve the performance of time delay estimation, especially when using coarse mesh. It is worth noting that the proposed algorithm can be applied not only to OFDM systems, but also to any communication system with multi-carrier characteristics.

REFERENCES

[1] R. van Nee and R. Prasad, *OFDM for Wireless Multimedia Communications*. Norwood, MA, USA: Artech House, 2000.
[2] H. Ni, G. Ren, and Y. Chang, "A TDOA location scheme in OFDM based WMANs," *IEEE Trans. Consum. Electron.*, vol. 54, no. 3, pp. 1017–1021, Aug. 2008.
[3] R. J. Anderson and R. S. Mia, "Location of wideband OFDM transmitters with limited receiver bandwidth," U.S. Patent 7 844 280 B2, Nov. 30, 2010.
[4] A. Makki, A. Siddig, M. M. Saad, J. R. Cavallaro, and C. J. Bleakley, "High-resolution time of arrival estimation for OFDM-based transceivers," *Electron. Lett.*, vol. 51, no. 3, pp. 294–296, Feb. 2015.
[5] L. Ying and S. Wang, "TOA estimation method using fourth order cumulants," in *Proc. Int. Conf. Signal Process.*, 2000, pp. 210–214.
[6] Y.-T. Chan, H. Y. C. Hang, and P.-C. Ching, "Exact and approximate maximum likelihood localization algorithms," *IEEE Trans. Veh. Technol.*, vol. 55, no. 1, pp. 10–16, Jan. 2006.
[7] G. Wang and H. Chen, "An importance sampling method for TDOA-based source localization," *IEEE Trans. Wireless Commun.*, vol. 10, no. 5, pp. 1560–1568, May 2011.
[8] J. Li, Y. J. Zhao, and D.-H. Li, "Time delay estimation using Markov Chain Monte Carlo method," *Acta Phys. Sinica-Chin. Ed.*, vol. 63, no. 13, 2014, Art. no. 130701.
[9] T.-J. Shan, M. Wax, and T. Kailath, "On spatial smoothing for direction-of-arrival estimation of coherent signals," *IEEE Trans. Acoust., Speech, Signal Process.*, vol. 33, no. 4, pp. 806–811, Aug. 1985.
[10] X. Li and K. Pahlavan, "Super-resolution TOA estimation with diversity for indoor geolocation," *IEEE Trans. Wireless Commun.*, vol. 3, no. 1, pp. 224–234, Jan. 2004.
[11] M. Rudelson and R. Vershynin, "On sparse reconstruction from Fourier and Gaussian measurements," *Courant Inst. Math. Sci.*, vol. 61, no. 8, pp. 1025–1045, 2008.
[12] F. Wang and X. Zhang, "Joint estimation of TOA and DOA in IR-UWB system using sparse representation framework," *ETRI J.*, vol. 36, no. 3, pp. 460–468, 2014.
[13] Y. Yin, G. Qiao, S. Liu, and F. Zhou, "Sparse channel estimation of underwater acoustic orthogonal frequency division multiplexing based on basis pursuit denoising," *Acta Phys. Sinica-Chin. Ed.*, vol. 64, no. 6, 2015, Art. no. 64301.
[14] K. Zhi-Wei, W. Chun-Yan, L. Jin, M. Xin, and G. Ming-Zhen, "Pulsar time delay estimation method based on two-level compressed sensing," *Acta Phys. Sinica*, vol. 67, no. 9, Aug. 2018, Art. no. 099701.
[15] J. Fang, F. Wang, Y. Shen, H. Li, and R. S. Blum, "Super-resolution compressed sensing for line spectral estimation: An iterative reweighted approach," *IEEE Trans. Signal Process.*, vol. 64, no. 18, pp. 4649–4662, Sep. 2016.
[16] M. E. Tipping, "Sparse Bayesian learning and the relevance vector machine," *J. Mach. Learn. Res.*, vol. 1, pp. 211–244, Sep. 2001.
[17] D. P. Wipf and S. S. Nagarajan, "A new view of automatic relevance determination," in *Proc. Adv. Neural Inf. Process. Syst.*, 2008, pp. 1625–1632.
[18] D. P. Wipf and B. D. Rao, "An empirical Bayesian strategy for solving the simultaneous sparse approximation problem," *IEEE Trans. Signal Process.*, vol. 55, no. 7, pp. 3704–3716, Jul. 2007.
[19] Z. Yang, L. Xie, and C. Zhang, "Off-grid direction of arrival estimation using sparse Bayesian inference," *IEEE Trans. Signal Process.*, vol. 61, no. 1, pp. 38–43, Jan. 2013.
[20] J. Dai, A. Liu, and V. K. N. Lau, "FDD massive MIMO channel estimation with arbitrary 2D-array geometry," *IEEE Trans. Signal Process.*, vol. 66, no. 10, pp. 2584–2599, May 2018.
[21] W. C. Jakes and D. C. Cox, *Microwave Mobile Communications*. Hoboken, NJ, USA: Wiley, 1994.
[22] S. S. Chen, D. L. Donoho, and M. A. Saunders, "Atomic decomposition by basis pursuit," *SIAM Rev.*, vol. 43, no. 1, pp. 129–159, 2001.
[23] R. Tibshirani, "Regression shrinkage and selection via the lasso," *J. Roy. Stat. Soc. B (Methodol.)*, vol. 58, no. 1, pp. 267–288, 1996.
[24] H. Zhu, G. Leus, and G. B. Giannakis, "Sparsity-cognizant total least-squares for perturbed compressive sampling," *IEEE Trans. Signal Process.*, vol. 59, no. 5, pp. 2002–2016, May 2011.
[25] C. Darwin, *Origin of Species by Means of Natural Selection: Or the Preservation of Favored Races in the Struggle for Life*. New York, NY, USA: Collier, 1901.
[26] R. M. Neal, *Bayesian Learning for Neural Networks*. New York, NY, USA: Springer, 1996.
[27] S. C. Choi, "Iterative methods for singular linear equations and least-squares problems," Ph.D. dissertation, Stanford Univ., Stanford, CA, USA, 2006.
[28] G. McLachlan and T. Krishnan, *The EM Algorithm and Extensions*. New York, NY, USA: Wiley, 1997.
[29] D. P. Wipf and B. D. Rao, "Sparse Bayesian learning for basis selection," *IEEE Trans. Signal Process.*, vol. 52, no. 8, pp. 2153–2164, Aug. 2004.
[30] Y.-H. Zhou, F. Tong, and G. -Q. Zhang, "Distributed compressed sensing estimation of underwater acoustic OFDM channel," *Appl. Acoust.*, vol. 117, pp. 160–166, Feb. 2017.
[31] M. S. Gast, *802.11 Wireless Networks: The Definitive Guide*. Sebastopol, CA, USA: O'Reilly Associates, 2002.

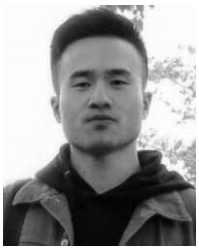

PENG ZHANG received the B.S. degree from PLA Strategic Support Force Information Engineering University (SSFIEU), Zhengzhou, China, in 2016, where he is currently pursuing the M.S. degree in communications and information system. His main research interests include wireless communication theory, signal processing, and parameter estimation.

ZI-RU ZHENG received the B.S. degree from PLA Strategic Support Force Information Engineering University (SSFIEU), Zhengzhou, China, in 2016. He is currently working in communications and information system with Unit 78118 of PLA, Chengdu, China. His main research interest includes wireless communication theory.

WEI-JIA CUI received the M.S. and Ph.D. degrees from PLA Strategic Support Force Information Engineering University (SSFIEU), Zhengzhou, China, in 2001 and 2007, respectively, where he is currently working in communications and information system. His main research interests include wireless communication theory, satellite and mobile communication, and signal processing.

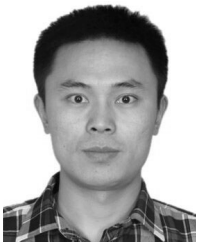

BIN BA was born in 1987. He received the M.S. and Ph.D. degrees from PLA Strategic Support Force Information Engineering University (SSFIEU), Zhengzhou, China, in 2012 and 2015, respectively, where he is currently working in communications and information systems. His main research interests include wireless communication theory, signal processing, and parameter estimation.